

Reaction Dynamics Around Coulomb Barrier With Weakly Bound Nuclei

Vivek Vijay Parkar

Nuclear Physics Division

Vivek Vijay Parkar is the recipient of the Indian National Science Academy Award for the year 2015

Abstract

The effect of weakly bound structure and low separation energies in ${}^6\text{Li}$ and ${}^9\text{Be}$ nuclei on different reaction mechanisms, *viz.*, elastic scattering and fusion reaction is studied in detail with large number of targets at energies around the Coulomb barrier. It is observed that the inclusion of breakup channel brought in by these weakly bound nuclei is playing a major role in different reaction channels in a given nuclear reaction.

Introduction

In recent years, the study of the reaction dynamics involving weakly bound nuclei has become one of the most intriguing and challenging problems in low energy nuclear physics [1]. The interest in understanding the influence of break-up on other reaction channels has indeed received a fillip in recent years, especially because of the recent advent of radioactive ion beam (RIB) facilities in different laboratories around the world. These RIB facilities can accelerate the nuclei away from line of stability (weakly bound unstable/exotic nuclei), which is not possible from conventional particle accelerators. The understanding of the fusion process using RIB has a great impact on the production of super heavy elements and in reactions of astrophysical interest. At present, as the intensities and beam resolution of RIBs are limited, it is difficult to carry out precision measurements using RIBs. Hence experiments with stable weakly bound projectiles like ${}^6\text{Li}$ and ${}^9\text{Be}$ are very important in understanding the various reaction mechanisms, *viz.*, the effect of breakup on the fusion process, significance of incomplete fusion etc. The study of reactions induced by such weakly bound stable nuclei would provide a basis to understand the reaction mechanisms of weakly bound unstable nuclei. Such reactions provide the platform to establish the best experimental techniques and reaction models required for the best study of exotic nuclei available at RIB facilities with low intensities.

The small separation energies e.g., ${}^7\text{Li} \rightarrow \alpha + t$, $S_{\alpha,t} = 2.47$ MeV, ${}^6\text{Li} \rightarrow \alpha + d$, $S_{\alpha,d} = 1.47$ MeV, ${}^9\text{Be} \rightarrow \alpha + {}^5\text{He}$, $S_{\alpha,{}^5\text{He}} = 2.47$ MeV etc., suggests that these nuclei can easily break in the nuclear or Coulomb field, which in turn can

influence the scattering and/or reaction cross-sections. With this in view, we have carried out several investigations to understand the reaction mechanisms involving these stable weakly bound projectiles on a range of target nuclei. Some of the important results are discussed in this report.

Precision measurement of elastic scattering in ${}^7\text{Li}$, ${}^9\text{Be} + {}^{208}\text{Pb}$ reactions below Coulomb barrier energies for investigation of dipole polarizability and cluster structure:

The Coulomb field due to the target nucleus induces a dipole moment in the projectile. The interaction of the electric field with the projectile dipole moment leads to a polarization potential which is attractive. As a result the Coulomb potential gets reduced and which in turn modifies the elastic scattering at energies below the Coulomb barrier. By measuring the small but measurable deviation from pure Coulomb scattering arising due to dipole moment of the projectile, it is possible to determine the dipole polarizability of the projectile. With this in mind, we have carried out high precision elastic scattering measurements for ${}^7\text{Li}$ and ${}^9\text{Be}$ scattering from ${}^{208}\text{Pb}$ at several energies both deep below and around the Coulomb barrier.

Dipole polarizability of a nucleus arises due to the fact that during a collision between two nuclei, the presence of strong electric field distorts the charge distribution of the nuclei as protons and neutrons are forced to move in opposite direction resulting in an additional interaction that modifies the Coulomb potential. As the dipole operator leads to transition between states of opposite parity and for normal nuclei, states of opposite parity are at high excitation energy, the effect of the coupling

between these states and hence dipole polarizability is very small for such strongly bound nuclei. For weakly bound nuclei due to low breakup threshold, continuum states of opposite parity are nearby which helps in excitation to these levels, e.g., in case of ${}^7\text{Li}$ with breakup threshold of only 2.47 MeV, positive parity $\alpha+t$ breakup states can couple to negative parity ground state via dipole operator. Theoretically the dipole polarizability parameter, α is defined as,

$$\alpha = \frac{8\pi}{9} \sum_{n \neq 0} \frac{B(E1, g.s. \rightarrow n)}{(E_n - E_0)}$$

which suggests that this parameter is strongly depending on $B(E1)$ value. Here E_n corresponds to the energy of the discretized state 'n' which is in continuum. Experimentally, the role of electric dipole polarizability (α) can be investigated by accurate measurement of elastic scattering of such weakly bound nucleus in the field of a heavy nucleus. This effect is quantified in terms of deviation from pure Rutherford scattering.

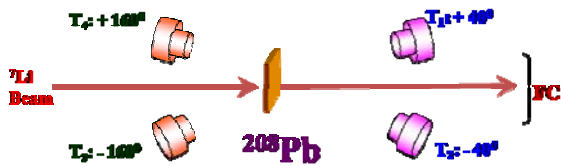


Fig. 1: Schematic illustration of experimental setup for the precise measurement of elastic scattering in ${}^7\text{Li}, {}^9\text{Be}+{}^{208}\text{Pb}$ reaction.

With this aim, measurements of elastic scattering cross-section of ${}^7\text{Li}$ from ${}^{208}\text{Pb}$ have been performed at energies from 18 to 28 MeV (Coulomb barrier ~ 30 MeV). A high precision measurement (statistical error $< 0.5\%$) was achieved by measuring double ratio (thereby avoiding various systematical errors)

$$R = \frac{\sigma(E_1, \theta_1) / \sigma(E_1, \theta_2)}{\sigma(E_2, \theta_1) / \sigma(E_2, \theta_2)} = \frac{C(E_1, \theta_1) / C(E_1, \theta_2)}{C(E_2, \theta_1) / C(E_2, \theta_2)}$$

where, E_1, E_2 are two bombarding energies and θ_1 and θ_2 are two scattering angles. $C(E, \theta)$ is the number of counts recorded in the detector at energy E and angle θ . In this experiment, $\theta_1 = 400, \theta_2 = 1600$ and $E_1 < E_2$ ($E_1 = 16$ MeV and $E_2 = 18 - 28$ MeV). Two such identical telescopes were placed symmetrically to the left and right of the incident beam at ± 400 and ± 1600 to eliminate, in the first order, possible beam wandering. The schematic of experimental setup is given in Fig. 1. The measured ratio was plotted as a function of incident energy which showed the deviation from $R = 1$.

The Continuum Discretized Coupled Channel (CDCC) calculations, which take into account the unbound states of the projectile and coupling with the ground state, were performed to explain this ratio, and the value of dipole polarizability extracted. ${}^7\text{Li}$ was assumed to have $\alpha+t$ cluster structure with the well-known $\alpha-t$ binding potential and couplings were included between ground state, inelastic state of ${}^7\text{Li}$ and the resonant and non-resonant continuum states. The non-resonant continuum states above breakup threshold were discretised into momentum bins of width 0.25 fm^{-1} with respect to the momentum of the $\alpha+t$ relative motion. The wave functions for the continuum bins were normalized to unity. Each bin was treated as an excited state of ${}^7\text{Li}$ with E_x equal to the mean bin energy. The scattering wave functions were then calculated at this energy and energy independence within the bin was assumed. For $\alpha+{}^{208}\text{Pb}$ and $t+{}^{208}\text{Pb}$ potential, required for cluster folding form factor calculations, global optical potentials evaluated at four- and three-seventh of the projectile energy were used. A energy-dependent renormalisation factor was built-in from fitting the existing data at slightly higher energies on elastic and fusion cross section simultaneously which was then extrapolated to the energy of interest. Best agreement between the data and CDCC calculations was obtained and the value of the dipole polarizability ($\alpha=0.045 \text{ fm}^3$) extracted [2]. In Fig. 2, comparison between measured ratio with CDCC calculations is shown for ${}^7\text{Li}+{}^{208}\text{Pb}$ reaction.

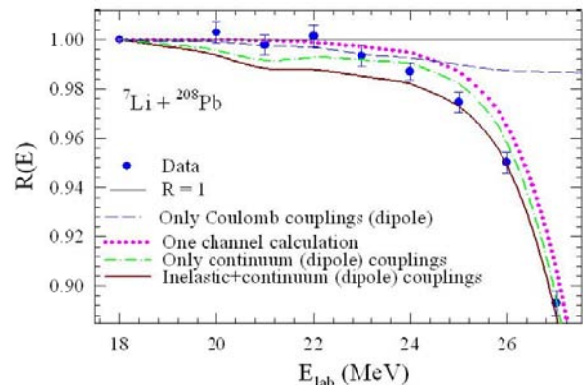


Fig 2: Comparison of measured ratio with CDCC calculations in ${}^7\text{Li}+{}^{208}\text{Pb}$ reaction

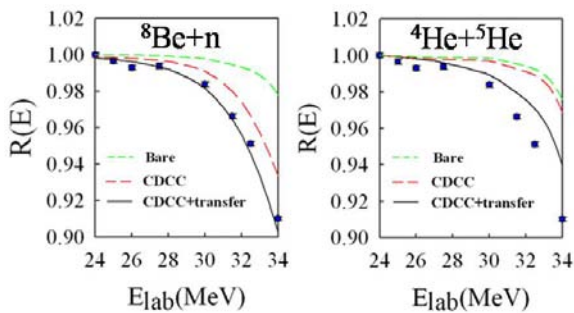


Fig 3: Measured ratio with CDCC calculations in ${}^9\text{Be}+{}^{208}\text{Pb}$ reaction assuming two cluster structures ${}^8\text{Be}+n$ and ${}^4\text{He}+{}^5\text{He}$

Similar precision elastic scattering measurements and CDCC calculations were also performed for ${}^9\text{Be}+{}^{208}\text{Pb}$ reaction. The two cluster structures of ${}^9\text{Be}$, namely ${}^4\text{He}+{}^5\text{He}$ and $n+{}^8\text{Be}$ were used in two independent CDCC calculations along with neutron transfer channel. It is observed that the $n+{}^8\text{Be}$ structure (see Fig. 3) is more appropriate in comparison to ${}^4\text{He}+{}^5\text{He}$ structure for explaining the data over a large energy range [3].

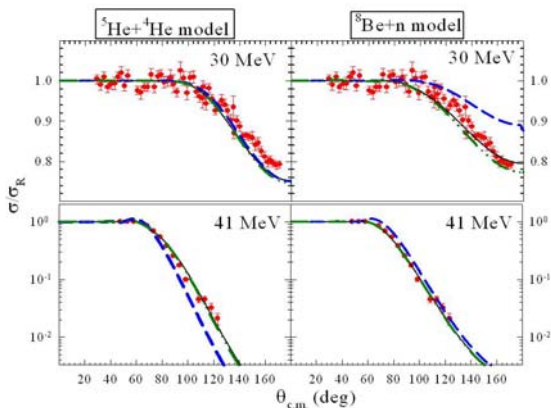


Fig. 4: The comparison of measured elastic scattering data for ${}^9\text{Be}+{}^{28}\text{Si}$ reaction with coupled channels calculations from two models: ${}^5\text{He} + {}^4\text{He}$ (left column) and ${}^8\text{Be} + n$ (right column)

To validate these two cluster structures of ${}^9\text{Be}$, we have also considered the available elastic scattering angular distribution data with ${}^{28}\text{Si}$, ${}^{64}\text{Zn}$, and ${}^{144}\text{Sm}$ targets. The results of the calculations suggest that the breakup coupling effects are significant for the ${}^4\text{He}+{}^5\text{He}$ cluster model above the barrier energies, while they are dominant at relatively lower energies for the ${}^8\text{Be} + n$ model. The addition of a one-neutron stripping channel in the ${}^8\text{Be} + n$ model gives an overall good description of the elastic data for all the systems considered [3]. In Fig. 4, the measured elastic scattering angular distribution data for ${}^9\text{Be}+{}^{144}\text{Sm}$ reaction is shown along with calculations using two cluster structures.

Fusion cross-sections in ${}^6\text{Li}$ and ${}^9\text{Be}$ induced reactions:

Fusion of two colliding nuclei around the Coulomb barrier is a complex phenomenon. Quantum mechanical barrier penetration occurs in a multidimensional space and coupling to the internal degrees of freedom of the participating nuclei plays an important role. There are several interesting features associated with the fusion process. Experimentally measured sub-barrier fusion cross sections for tightly bound nuclei are enhanced by several orders of magnitude over the predictions of the simple one-dimensional barrier penetration models (1DBPM). The observed enhancement is understood in terms of couplings to the low-lying collective excited states of target and projectile and to transfer of one or more nucleons. Understanding the fusion process with weakly bound nuclei, either stable or short-lived, brings in a new set of challenges. To start with, the definition of fusion cross section itself needs to be clarified. There are similar processes such as the incomplete fusion (ICF), wherein only part of the projectile fuses with the target. Hence, a distinction needs to be made wherever possible between complete fusion (CF), which involves the fusion of the projectile as a whole with the target, and total fusion (TF), which also includes the ICF component. The fusion reactions with weakly bound stable/unstable nuclei are of astrophysical interest and can give insight for super heavy element production. As far as the spectroscopy point of view is concerned, fusion evaporation reactions are the usual way to get the high spin structure of excited nuclei. In addition, weakly bound nuclei like ${}^6\text{Li}$, ${}^9\text{Be}$, ${}^{10,11}\text{B}$ beams are ideal for studying high spin states of stable and neutron rich nuclei produced through ICF reactions.

In the case of reactions where at least one of the colliding nuclei has a sufficiently low binding energy, the break-up becomes an important process. This break-up, if considered as a loss of flux from the incident channel, then it should suppress the fusion cross-sections, but if considered as one more channel for coupling in addition to transfer or inelastic, then it is supposed to enhance the fusion cross-section at below Coulomb barrier energies. We have performed several fusion cross-section measurements with stable weakly bound ${}^6\text{Li}$ and ${}^9\text{Be}$ nuclei on several targets viz., ${}^{89}\text{Y}$, ${}^{90}\text{Zr}$, ${}^{124}\text{Sn}$, ${}^{159}\text{Tb}$, ${}^{144,152}\text{Sm}$, ${}^{197}\text{Au}$, ${}^{198}\text{Pt}$ etc. Mainly two methods of online and/or offline gamma ray measurement techniques are utilized to extract the evaporation residue (ER) and hence fusion cross-sections. In Fig. 5 (A-C), one of the

examples for each projectile is shown along with coupled channels (CC) calculations. The measured CF cross-sections are found to be suppressed at above barrier energies by $\sim 32\%$, 26% , and 28% for ${}^6\text{Li}$, ${}^7\text{Li}$ and ${}^9\text{Be}$ respectively w.r.t. CC calculations [5-7]. In Fig. 5 (A) and (C), we have also shown the comparison with the fusion cross-sections from tightly bound nuclei forming the

similar compound nucleus, which also confirms the suppression. In Fig. 5 (D), we have plotted the systematic of this suppression factor (FCF) w.r.t. the product of projectile and target charge ($Z_p \cdot Z_T$) which shows (i) For a particular projectile, the suppression factor is more or less independent of the product $Z_p \cdot Z_T$ and (ii)

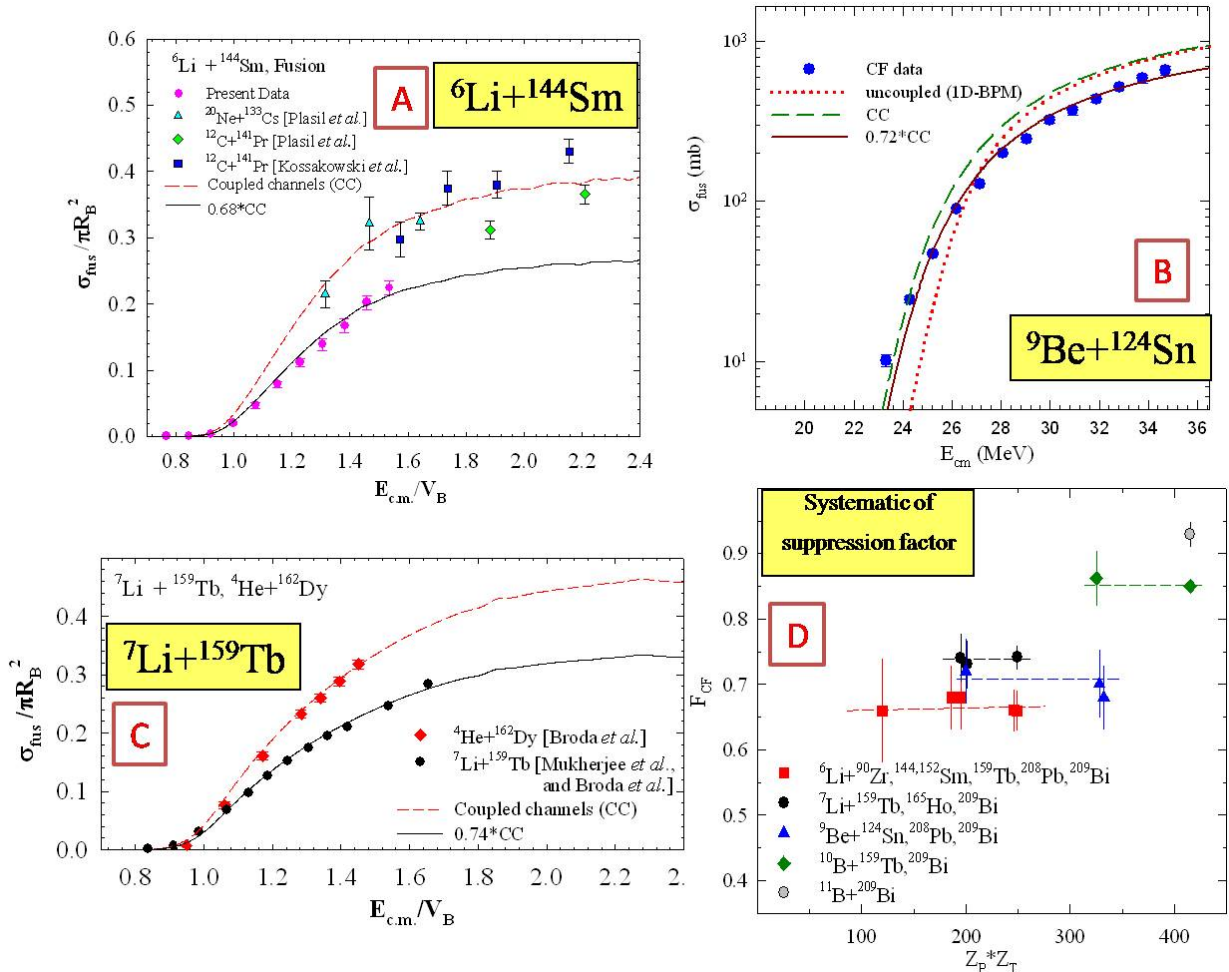


Fig 5: Measured Complete Fusion (CF) cross-sections for (A) ${}^6\text{Li} + {}^{144}\text{Sm}$ (B) ${}^9\text{Be} + {}^{124}\text{Sn}$ (C) ${}^7\text{Li} + {}^{159}\text{Tb}$ were compared with Coupled Channel calculations. The obtained suppression factor for 6Li, 7Li, 9Be is following the systematic w.r.t. $Z_p \cdot Z_T$ as shown in (D). See text for details.

Suppression increases with decreasing breakup threshold of the projectile [5].

Summary and Conclusion:

We have performed high precision elastic scattering measurements over a range of energies, from sub-barrier to near barrier for ${}^7\text{Li}, {}^9\text{Be} + {}^{208}\text{Pb}$ reactions. The ratio method of forward to backward elastic scattering events ruled out all the systematic errors of the measurement. The statistical accuracy obtained was close to 0.5%. The

CDCC calculations have been performed and the dipole polarizability parameter was extracted. Also in the case of ${}^9\text{Be}$, cluster structure of $8\text{Be} + n$ is found to be favorable over ${}^4\text{He} + {}^5\text{He}$ structure.

In the study of fusion of weakly bound nuclei with range of targets, we observed that the complete fusion cross-sections are suppressed compared to the CC calculations. We have plotted the systematic of the observed suppression factor w.r.t. charge product of projectile and

target (ZP^*ZT). The suppression factor (FCF) for a particular projectile is found to be independent of ZP^*ZT . The suppression increases with decreasing the breakup threshold.

In the near future, the rapid development of upcoming Radioactive Ion Beam facilities, viz., FAIR and SPIRAL2, will provide more weakly bound unstable nuclei away from the line of stability, for which one can extend similar kind of study of dipole polarizability as well as cluster structure to great detail using these precision elastic scattering measurements. The systematic of fusion suppression observed with stable weakly bound nuclei can be extended in studies with these Radioactive Ion Beams.

Acknowledgement:

I am grateful to all the collaborators for help and support at various stages during this research work. I also acknowledge the Pelletron-LINAC accelerator staff at TIFR, Mumbai for giving excellent quality of beam during this research.

References

1. L.F. Canto et al., Phys. Rep. 596, 1 (2015)
2. V.V. Parkar et al., Phys. Rev. C 78, 021601(R) (2008)
3. S. K. Pandit et al., Phys. Rev. C 84, 031601(R) (2011)
4. V.V. Parkar et al., Phys. Rev. C 87, 034602 (2013)
5. V.V. Parkar et al., Phys. Rev. C 82, 054601 (2010)
6. P. K. Rath et al., Phys. Rev. C 79, 051601(R) (2009)
7. V. Jha, V. V. Parkar, S. Kailas, Phys. Rev. C 89, 034605 (2014)